Structure of Chemisorbed Sulfur on a Pt(111) Electrode

Y.-E. Sung,[†] W. Chrzanowski,[†] A. Zolfaghari,[‡] G. Jerkiewicz,[‡] and A. Wieckowski*,[†]

Contribution from the Department of Chemistry, University of Illinois and Frederick Seitz Materials Research Laboratory, 600 S. Mathews Ave., Urbana, Illinois 61801, and Département de Chimie, Université de Sherbrooke, Sherbrooke, Québec, J1K 2R1, Canada

Received July 30, 1996[⊗]

Abstract: Electron spectroscopic and diffraction results obtained in ultra-high-vacuum, combined with cyclic voltammetric data, are reported for sulfur adlayers deposited from aqueous sulfide and bisulfide media on Pt(111). The highest coverage obtained by Auger electron spectroscopy, 0.94 ± 0.05 monolayer, is very close to the coverage obtained from coulometry, and is associated with a (1×1) surface phase. This coverage is much higher than that obtained in previous electrochemical studies but is the same as found by other investigators using S_2 beam dosing in vacuum. The near complete sulfur monolayer is characterized by a rapid and incomplete oxidation in a narrow potential range near 0.70 V vs a Ag/AgCl reference. Neither full sulfur monolayer coverage nor a sharp voltammetric transition could be obtained when traces of oxygen were present in the electrochemical cell. Oxidation of the (1×1) adlayer (at $\approx$1 monolayer) gave rise to a previously unreported (2×2) structure, at $^1/_2$ monolayer. Further voltammetric stripping resulted in two more adlattices: $(\sqrt{3}\times\sqrt{3})R30°$ at $^1/_3$ monolayer and p(2×2) at $^1/_4$ monolayer, as reported in previous gas phase studies. The selective stripping procedure provides unique electrochemical control at room temperature of surface structure and coverage, without any change in the long-range surface order of the substrate. When dosing was carried out from bisulfide solution, a $(\sqrt{3}\times\sqrt{7})$ phase at $^3/_5$ monolayer was formed, which once again was not reported previously. The results of the core-level electron energy loss spectroscopy studies suggest that sulfur adatoms retain some of the negative charge and that this charge plays a major role in controlling hydrogen adsorption coverage in the presence of coadsorbed sulfur on Pt(111).

1. Introduction

Sulfur adsorption and its significance vs modifying the properties of metal electrodes is broadly recognized.[1−17] On practically all metals investigated sulfur blocks surface sites and restricts access of other species that either would be adsorbed or decomposed.[4,6,8,11−13,17] However, while inhibiting hydrogen adsorption and evolution, preadsorbed sulfur strongly promotes the absorption of hydrogen into metal lattices.[6,14,17−19] That is, it exhibits a dual action with respect to hydrogen interfacial transfer. Investigating such a behavior is directly relevant in metal-hydride-battery[20] and hydrogen-embrittlement research.[21,22] The presence of chemisorbed sulfur also accelerates anodic dissolution of several metals and alloys[23−25] and retards their passivation.[26] The first effect is most probably due to sulfur-induced weakening of the metal−metal bond,[23,24] and the second to interference by sulfur with OH^- anion adsorption, the precursor formed during passivation.[26] As an electronegative element, sulfur perturbs the work function on metal substrates.[27,28] Formation of the surface chemical bond between platinum and sulfur induces a large decrease in the density of 5d states[29] that has recently been correlated to reduction of platinum catalytic activity.[30−32] Despite these electronic effects

* Address correspondence to this author.
† University of Illinois and Frederick Seitz Materials Research Laboratory.
‡ Université de Sherbrooke.
⊗ Abstract published in *Advance ACS Abstracts,* December 15, 1996.

(1) Loucka, T. *J. Electroanal. Chem.* **1972**, *36*, 355.
(2) Ramasubramanian, N. *J. Electroanal. Chem.* **1975**, *64*, 21.
(3) Contractor, A. Q.; Lal, H. *J. Electroanal. Chem.* **1979**, *96*, 175.
(4) Oudar, J. *Catal. Rev.-Sci. Eng*. **1980**, *22*, 171−195.
(5) Szklarczyk, M.; Czerwinski, A.; Sobkowski, J. *J. Electroanal. Chem.* **1982**, *132*, 263.
(6) Marcus, P.; Oudar, J. In *Hydrogen Degradation of Ferrous Alloys*; Oriani, R. A., Hirth, J. P., Smialowski, M., Eds.; Noyes Publications: Park Ridge, NJ, 1985; Chapter 3, pp 36−77.
(7) Protopopoff, E.; Marcus, P. *Surf. Sci*. **1986**, *169*, L237−L244.
(8) Zurawski, D.; Chan, K. W. H.; Wieckowski, A. *J. Electroanal. Chem.* **1987**, *230*, 205−219.
(9) Batina, N.; McCargar, J. W.; Salaita, G. N.; Lu, F.; Laguren-Davidson, L.; Lin, C.-H.; Hubbard, A. T. *Langmuir* **1989**, *5*, 123−128.
(10) Mebrahtu, T.; Bothwell, M. E.; Harris, J. E.; Cali, G. J.; Soriaga, M. P. *J. Electroanal. Chem*. **1991**, *300*, 487−498.
(11) Protopopoff, E.; Marcus, P. *J. Chim. Phys*. **1991**, *88*, 1423−1452.
(12) Krauskopf, E. K.; Wieckowski, A. In *Adsorption of Molecules at Metal Electrodes*, Lipkowski, J., Ross, P. N., Eds.; VCH: New York, 1992; pp 119−169.
(13) Svetlicic, V.; Clavilier, J.; Zutic, V.; Chevalet, J.; Elachi, K. *J. Electroanal. Chem*. **1993**, *344*, 145−160.
(14) (a) Conway, B. E.; Jerkiewicz, G. *J. Electroanal. Chem.* **1993**, *357*, 47−66. (b) Conway, B. E.; Jerkiewicz, G. *Z. Phys. Chem. Bd.* **1994**, *183*, 281−286.
(15) Szynkarczuk, J.; Komorowski, P. G.; Donini, J. C. *Electrochim. Acta* **1995**, *40*, 487−494.
(16) Quijada, C.; Rodes, A.; Vazquez, J. L.; Perez, J. M.; Aldaz, A. *J. Electroanal. Chem.* **1995**, *398*, 105−115.
(17) Jerkiewicz, G.; Borodzinski, J. J.; Chrzanowski, W.; Conway, B. E. *J. Electrochem. Soc*. **1995**, *142*, 3755−3763.
(18) Iyer, R. N.; Pickering, H. W.; Zamanzadeh, M. *J. Electrochem. Soc*. **1989**, *136*, 2463−2470.
(19) (a) Jerkiewicz, G.; Zolfaghari, A. *J. Electrochem. Soc*. **1996**, *143*, 1240−1248. (b) Jerkiewicz, G.; Zolfaghari, A. *J. Phys. Chem*. **1996**, *100*, 8454−8461.
(20) Ovshinsky, S. R.; Fetcenko, M. A.; Ross, J. *Science* **1993**, *260*, 176−181.
(21) Flis, J., Ed. *Corrosion of Metals and Hydrogen-Related Phenomena*; Elsevier/PWN: Amsterdam, New York, Warsaw, 1991.
(22) Iyer, R. N.; Takeuchi, I.; Zamanzadeh, M.; Pickering, H. W. *Corrosion* **1990**, *46*, 460−468.
(23) Oudar, J.; Marcus, P. *Appl. Surf. Sci.* **1979**, *3*, 48−67.
(24) Marcus, P.; Tessier, A.; Oudar, J. *Corros. Sci.* **1984**, *24*, 259−268.
(25) (a) Suzuki, T.; Yamada, T.; Itaya, K. *J. Phys. Chem.* **1996**, *100*, 8954−8961. (b) Ando, S.; Suzuki, T.; Itaya, K. *J. Electroanal. Chem.* In press.
(26) Marcus, P.; Oudar, J. In *Passivity of Metals and Semiconductors*, Froment, M., Ed.; Elsevier: 1983, p 119.
(27) Billy, J.; Abon, M. *Surf. Sci*. **1984**, *146*, L525−L532.
(28) Kiskinova, M.; Goodman, D. W. *Surf. Sci.* **1981**, *108*, 64−76.
(29) Rodriguez, J. A.; Kuhn, M.; Hrbek, J. *Chem. Phys. Lett.* **1996**, *251*, 13−19.

S0002-7863(96)02637-6 CCC: $14.00

that depend on sulfur coverage and structure[27,29] and the "through-space" electrostatic lateral interactions,[33] the platinum−sulfur bond is predominantly covalent.[27]

Studies of sulfur adsorption from the gas phase on Pt(111) have revealed several distinctively different surface structures[34−41] that highlight a delicate balance of forces between adsorbate−adsorbate and adsorbate−metal surface systems.[41] The main structures observed by low electron energy diffraction under a variety of temperature and pressure conditions are as follows: p(2×2) at $^1/_4$ monolayer coverage, $(\sqrt{3}\times\sqrt{3})R30°$ at $^1/_3$ monolayer, and $\begin{bmatrix} 4 & -1 \\ -1 & 2 \end{bmatrix}$ at $^3/_7$ monolayer.[35,41] Streaks and diffuse reflections have also been observed. Using S_n (mainly S_2) beam generated from electrochemical decomposition of Ag_2S in UHV, Heegemann *et al*. reported a room temperature coverage close to a full 1.0-monolayer coverage,[35] the result recently confirmed by Rodriguez et al.[29] Second layer and physisorbed sulfur were concluded to be a part of this high coverage structure.[35] Each surface structure has its own desorption temperature, beginning not far above room temperature, and a complete sulfur desorption occurs at 1050 K.[35] Both atomic and molecular sulfur were found among the desorption products.[29] At $^1/_3$ monolayer and at lower coverage, sulfur is adsorbed on the fcc three-fold hollow sites.[29,37,41] There is also a bridge-site adsorption leading to S_2 desorption when the temperature is raised.[29]

In contrast to the rich structural chemistry of sulfur upon gas phase dosing conditions, only one structure of electrosorbed sulfur on Pt(111) was observed, $(\sqrt{3}\times\sqrt{3})R30°$.[9] In this paper, we provide evidence that several other structures can be obtained. Sulfur was deposited from aqueous sulfide and bisulfide media on Pt(111), and the interrogations were conducted by low electron energy diffraction (LEED), Auger electron spectroscopy (AES), and core-level electron energy loss spectroscopy (CEELS).[42−45] We correlate sulfur structure and cyclic voltammetry (CV) profiles, demonstrate a unique reactivity of the highly-packed sulfur adlayer under voltammetric conditions, and show effects of surface sulfur on hydrogen adsorption. We reference our CV data to the recent spectroscopic, thermal desorption, and molecular orbital results on sulfur adsorbed on Pt(111) from the gas phase.[29] To our knowledge, the comprehensive electrochemical study of sulfur adsorption and electrochemistry/gas phase adsorption comparisons, as those presented here, have not yet been reported. We also conclude that quantitative elimination of oxygen is a prerequisite of credible work on surface modification by sulfur and, most likely, by sulfur-containing species on platinum for a broad electrochemical use.

2. Experimental Section

The combined ultra-high-vacuum electrochemistry instrument that was used for this project has recently been reported.[44,45] The Ar ion bombardment/(oxygen) annealing cycles were repeated until appropriate order and cleanliness of the Pt(111) surface (Aremco) were confirmed by LEED and AES. The clean and ordered Pt(111) sample was transferred, without exposure to air, to the system antechamber for electrochemical measurements using conventional three-electrode circuitry, and the EG&G PAR 362 potentiostat. We used a primary beam of 3 and 0.5 kV for the AES and CEELS assays, in each case utilizing a Perkin Elmer PHI-10-155 cylindrical mirror electron energy analyzer. The electron energy loss spectra are presented in a differentiated mode (as obtained), or as integrated spectra. The integrated spectra were used to verify the peak position assignment, especially when the comparison was made between peak positions of S adsorbate and a Na_2S thin film.

The quantitative analysis of sulfur adlayers was performed using AES[44,45] and coulometry. Adsorption was carried out for 5 min. For the AES treatment, the thin film of Na_2S deposit was obtained by electrode emersion from a 30 mM Na_2S solution followed by water evaporation in UHV. The film was sufficiently thin to avoid surface charging but thick enough to screen AES transitions of platinum.[45] Such a thin film covered Pt(111) template was used as a standard for work with the sulfur adlayers.[45] The procedure involved a comparison of the peak-to-peak (p/p) ratio of sulfur at 153.0 eV relative to the Pt p/p ratio at 64.0 eV and the application of a set of AES quantitative equations recently reported from our group.[44,45] In the coulometric coverage measurements, a sulfur oxidation charge (q_i) was obtained by subtracting the oxide formation charge from the total anodic charge corresponding to platinum and sulfur oxidation. A summation of the net S oxidation charges for all CV sweeps until complete sulfur desorption ($q_S = \sum_i q_i$) gives a complete S oxidation charge.

All solutions were made of Millipore water (18 MΩ·cm). The supporting electrolyte, 0.10 M H_2SO_4, was prepared from ultra-pure grade sulfuric acid (GFS Chemicals). Na_2S (Johnson & Matthey) working solutions were made at concentrations of 1.0 and 10 mM to yield pH 11.0 and 12.0 solutions, respectively. Equivalent NaHS solutions had pH 9.0 and 9.5. Unless otherwise indicated all solutions were deaerated and blanketed with nitrogen (Linde, Oxygen Free, 99.99%) prior to the electrochemical studies. All measurements were conducted at room temperature. Electrode potentials are given vs Ag/AgCl reference with $[Cl^-] = 1.0$ M (the actual concentration of Cl^- in the UHV electrochemical cell was 1.0×10^{-5} M, and the potentials are re-calculated to the 1.0 M Cl^- concentration).

3. Results and Discussion

Surface Structure and Voltammetric Measurements. LEED (see Supporting Information) and cyclic voltammetry taken in 0.10 M H_2SO_4 solution (Figure 1, inset) demonstrate that the UHV-prepared Pt(111) surface is of high quality.[45−50] A Pt(111) electrode prepared in this manner was immersed in Na_2S working solutions for 5 min during which the rest potential was quite stable, at ca. 0.04 V. The sulfur-covered surface was rinsed 5 times with water and transferred either to UHV for

(30) Bartholomew, C. H.; Agrawal, P. K.; Katzer, J. R. *Advan. Catal.* **1982**, *31*, 135−242.
(31) Barbier, J.; Lamy-Pitara, E.; Marecot, P.; Boitiaux, J. P.; Cosyns, J.; Verna, F. *Adv. Catal.* **1990**, *37*, 279−318.
(32) Rodriguez, J. A.; Goodman, D. W. *Surf. Sci. Rep.* **1991**, *14*, 1−107.
(33) Lang, N. D.; Holloway, S.; Nørskov, J. K. *Surf. Sci.* **1985**, *150*, 24−38.
(34) Berthier, Y.; Perdereau, M.; Oudar, J. *Surf. Sci*. **1973**, *36*, 225−241.
(35) Heegemann, W.; Meister, K. H.; Bechtold, E.; Hayek, K. *Surf. Sci*. **1975**, *49*, 161−180.
(36) Astegger, St.; Bechtold, E. *Surf. Sci*. **1982**, *122*, 491−504.
(37) Hayek, K.; Glassl, H.; Gutmann, A.; Leonhard, H.; Prutton, M.; Tear, S. P.; Welton-Cook, M. R. *Surf. Sci*. **1985**, *152/153*, 419−425.
(38) (a) Koestner, R. J.; Salmeron, M.; Kollin, E. B.; Gland, J. L. *Surf. Sci.* **1986**, *172* 668−690. (b) Koestner, R. J.; Salmeron, M.; Kollin, E. B.; Gland, J. L. *Chem. Phys. Lett.* **1986**, *125*, 134−138.
(39) Kiskinova, M. P.; Szabo, A.; Yates, J. T., Jr. *Surf. Sci*. **1990**, *226*, 237−249.
(40) Sun, Y.-M.; Sloan, D.; Alberas, D. J.; Kovar, M.; Sun, Z.-J.; White, J. M. *Surf. Sci*. **1994**, *319*, 34−44.
(41) Yoon, H. A.; Materer, N.; Salmeron, M.; Van Hove, M. A.; Somorjai, G. A. *Surf. Sci.* In press.
(42) Hitchcock, A. P.; Tronc, M.; Modelli, A. *J. Phys. Chem*. **1989**, *93*, 3069−3077.
(43) (a) Cazaux J.; Coliiex, C. *J. Electron Spectrosc. Relat. Phenom*. **1990**, *52*, 837−853. (b) Cazaux, J.; Jbara, O.; Kim, K. H. *Surf. Sci*. **1991**, *247*, 360−374.
(44) (a) Mrozek, P.; Han, H.; Sung, Y.-E.; Wieckowski, A. *Surf. Sci*. **1994**, *319*, 21−33. (b) Sung, Y.-E.; Thomas, S.; Wieckowski, A. *J. Phys. Chem*. **1995**, *99*, 13513−13521.
(45) Thomas, S.; Sung, Y.-E.; Kim, H. S.; Wieckowski, A. *J. Phys. Chem.* **1996**, *100*, 11726−11735.
(46) Clavilier, J. *J. Electroanal. Chem*. **1980**, *107*, 211−216.
(47) Al Jaaf-Golze, K.; Kolb, D. M.; Scherson, D. *J. Electroanal. Chem.* **1986**, *200*, 353−362.
(48) Ross, P. N. *J. Chem. Phys*. **1991**, *88*, 1353−1380.
(49) Savich, W.; Sun, S.-G.; Lipkowski, J.; Wieckowski, A. *J. Electroanal. Chem*. **1995**, *388*, 233−237.
(50) Herrero, E.; Feliu, J. M.; Wieckowski, A.; Clavilier, J. *Surf. Sci*. **1995**, *325*, 131−138.

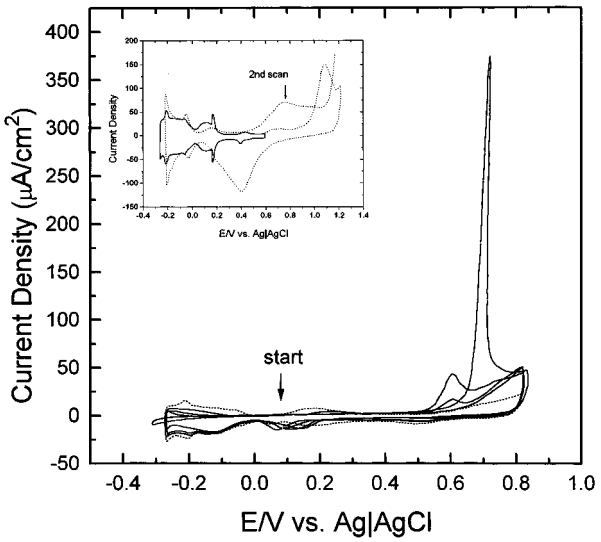

Figure 1. Cyclic voltammetry of the Pt(111) electrode in 0.10 M H_2SO_4: First voltammetric profile and successive voltammetric curves for S adsorbate oxidation. Sulfur was adsorbed from 1 mM Na_2S at the rest potential for 5 min. Scan rate 20 mV/s. Dotted curve refers to the voltammogram after the 20th cycle. Inset: Three cyclic voltammetric cycles of the Pt(111) electrode in 0.1 M H_2SO_4 in two electrode potential ranges, as shown.[45] Scan rate 50 mV/s.

surface characterization or to the electrochemical cell. The cell was filled out with 0.10 M H_2SO_4 electrolyte and the S adsorbate was characterized by voltammetry. In some experiments, the electrode potential was adjusted to several values in the range of electrochemical stability of surface sulfur on Pt(111)[9,11] and the electrode was emersed to UHV at a chosen potential.

A family of cyclic voltammograms of the S-covered Pt(111) electrode (in 0.10 M H_2SO_4 electrolyte) in the range of -0.28 to 0.82 V is shown in Figure 1. The first negative-going sweep shows an expected and complete suppression of hydrogen adsorption. Surprisingly, however, the first positive-going sweep displays a narrow, not yet reported peak at the onset of surface oxidation of platinum (at 0.70 V). Upon the sweep reversal, a small oxide reduction charge at ca. 0.50 V was found indicating that some surface sites were released during the positive-going scan. The LEED data obtained in parallel to the CV experiment demonstrate that the voltammetric spike corresponds to a transformation of the (1×1) to a (2×2) surface structure. (The thermodynamic origin of the sharp, near δ-function voltammogram separating the two different surface structures[51] will further be investigated.) The subsequent coulometric analysis (Experimental Section) based upon the well-known reaction stoichiometry involving six electrons per one S-adsorbate,[9,10]

$$Pt{-}S_{ads} + 4H_2O \rightarrow Pt + SO_4^{2-} + 8H^+ + 6e \qquad (1)$$

indicates that the (1×1) structure corresponds to near full monolayer coverage (0.94 ± 0.05 and 0.89 ± 0.05 monolayer in 1.0 and 10 mM Na_2S solutions, respectively). The coulometry also shows that the voltammetric oxidation during the first scan reduces the coverage approximately by half (to 0.47 ± 0.03 monolayer). Therefore, the surface structure obtained after the first voltammetric cycle is (2×2) at $^1/_2$ monolayer. After the second cycle, the sulfur coverage was reduced to 0.28 ± 0.02 monolayer, after the third, to 0.17 ± 0.03 monolayer, and after the fourth, to 0.09 ± 0.02 monolayer. These quantitative conclusions are corroborated by AES data (see below), and all the results are summarized in Tables 1 and 2. The corresponding LEED patterns are as follows: $(\sqrt{3}\times\sqrt{3})R30°$ after the second sweep (stable in the range from 0.25 to 0.38 monolayer); p(2×2) at 0.25 monolayer, after the third sweep; a weak (2×2) after the fourth sweep, and finally Pt(111)(1×1) (Table 1). That is, in contrast to previous work that showed only a $(\sqrt{3}\times\sqrt{3})R30°$ surface structure,[9] our work shows much richer structural chemistry. Whereas no noticeable surface disorder was found during the first cycles, the profile after 20 sweeps showed CV features representative of a partially disordered Pt(111) surface. This shows that cycling of Pt(111) in the range of -0.3 to 0.8 V cannot continue for too long without surface disorder. However, the fact that no disorder was found upon the first cycles is encouraging for the type of structural research we report here and for further work with S adsorbate on well-defined electrodes.

We also found that the narrow and sharp oxidation peak presented in Figure 1 could only be observed when oxygen-free Na_2S solutions were used for obtaining the S adsorbate. If electrochemical adsorption of sulfur was carried out in solutions exposed to air or under inert gas atmosphere with traces of oxygen, the narrow voltammetric feature disappeared and was replaced by a broad CV oxidative wave. The maximum coverage then was quite low, 0.64 ± 0.05 monolayer (from AES) and the structure was faint Pt(111)$(\sqrt{3}\times\sqrt{3})R30°$, rather than the (1×1) at ≈1 monolayer.

We conducted control measurements to check if the electrode emersion and system evacuation caused any detectable desorption or rearrangement to the S adlayer. In this series, the Pt(111)(1×1) S sample was transferred to UHV, LEED and AES-analyzed for 20 min, and brought back to the electrolyte for voltammetric characterization. The CV obtained in this manner was next compared with the one produced without the UHV exposure and characterization in the electron beam. We found that the voltammetric morphology between the two experiments was practically identical, and sulfur oxidation charges were the same within 3%, which falls within the experimental error. We conclude that the sulfur adsorbate on Pt(111) is stable in UHV and is unaffected by the electron beam exposure under the conditions meeting our surface analytical requirements.

To compare our data with the results of previous gas-phase investigations, the S-covered electrode covered by a near complete sulfur monolayer (at 0.94 monolayer) was subject to heat treatment. After brief heating of the (1×1) S surface to 900 and 1300 K, the LEED patterns were $(\sqrt{3}\times\sqrt{3})R30°$ at $^1/_3$ monolayer and p(2×2) at $^1/_4$ monolayer, respectively. We could not find in either the electrochemical or thermal studies the Heegemann's $\begin{bmatrix} 4 & -1 \\ 2 & -1 \end{bmatrix}$ adlattice with the coverage of $^3/_7$ monolayer.[35]

Voltammetric features obtained in 0.10 M H_2SO_4 after S adsorption from 1.0 mM NaHS solution are shown in Figure 2. The oxidation peak is broader than that obtained in Na_2S, and the sulfur coverage is only 0.62 ± 0.04 monolayer (or $^3/_5$ monolayer, Table 2). Notably, using NaHS solution gives us a not-yet-reported surface sulfur structure, $(\sqrt{3}\times\sqrt{7})$ (Figure 3). The lower coverage we report obtained with NaHS than with Na_2S reflects the distribution of H_2S Brønsted forms in solution;[52] evidently the anionic HS^- form is more surface active that the molecular $H_2S_{aq.}$ form. After the first and the second stripping cycles of the NaHS pretreated surface we obtained the p(2×2) structure, at the coverage of 0.21 ± 0.02 monolayer,

(51) (a) Collins, J. B.; Sacramento, P.; Rikvold, P. A.; Gunton, J. D. *Surf. Sci.* **1989**, *221*, 277−298. (b) Rikvold, P. A.; Wieckowski, A. *Phys. Scr.* **1992**, *T44*, 71−76.

(52) Cotton, F. A.; Wilkinson, G. *Advanced Inorganic Chemistry*, 4th ed.; John Wiley & Sons: New York, 1980; p 512.

Table 1. Sulfur Coverage and Structure Obtained in 1 mM Na_2S at Rest Potential on the Pt(111) Electrode after the Indicated Number of Oxidative CV Cycles (See Text)

no. of cycles	total charge, coulometry[a] (μC/cm^2)	coverage from coulometry[b] monolayer	coverage from AES monolayer	coverage from LEED monolayer	LEED structures
0	1365	0.94	0.95	1.0	(1×1)
1	682	0.47	0.44	0.5	(2×2) at $^1/_2$ monolayer
2	407	0.28	0.31	0.33	$(\sqrt{3}\times\sqrt{3})R30°$
3	247	0.17	0.22	0.25	p(2×2) at $^1/_4$ monolayer
4	131	0.09	0.10	<0.25	weak (2×2)
20	0	~0	0.02	0	(1×1)

[a] Net sulfur oxidation charge obtained by subtracting surface oxidation charge from the total charge. [b] Assuming 6 electron process per one surface sulfur adatom and 242 μC/cm^2 per 1e surface redox reaction at the Pt(111) electrode.[9,10]

Table 2. Sulfur Coverage and Structure Obtained in 1 mM NaHS at Rest Potential on the Pt(111) Electrode after the Indicated Number of Oxidative CV Cycles (See Text)

no. of cycles	total charge, coulometry[a] (μC/cm^2)	coverage from coulometry[b] monolayer	coverage from AES monolayer	coverage from LEED monolayer	LEED structures
0	901	0.62	0.70	0.6	$(\sqrt{3}\times\sqrt{7})$
1	302	0.21	0.24	0.25	p(2×2) at $^1/_2$ monolayer
2	117	0.08	0.11	<0.25	weak (2×2)

[a] Net sulfur oxidation charge obtained by subtracting surface oxidation charge from the total charge. [b] Assuming 6 electron process per one surface sulfur adatom and 242 μC/cm^2 per 1e surface redox reaction at the Pt(111) electrode.[9,10]

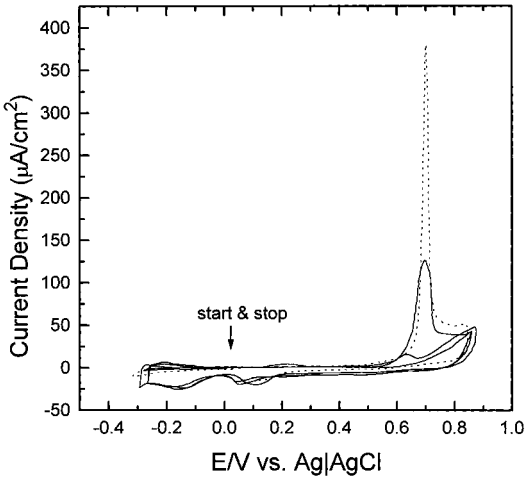

Figure 2. Cyclic voltammetry of Pt(111) in 0.10 M H_2SO_4. Solid lines: successive cycles for sulfur adsorbed from 1 mM NaHS at the rest potential for 5 min. Dotted line: contrasting data taken from Figure 2 (first cycle) with 1 mM Na_2S adsorption. Scan rate 20 mV/s.

and yet another poorly developed (2×2) structure, with the coverage of 0.08 ± 0.01 monolayer (Table 2). This indicates that surface sulfur forms ordered islands in UHV of sufficient coherence length for electron diffraction.[53]

We notice here that voltammetry demonstrates that there are two dissimilar forms of surface sulfur, one giving rise to a sharp voltammetric transition at 0.70 V and another, previously observed by many investigators, oxidized in a broad electrode potential range that roughly coincides with the potential range of platinum oxidation. As determined by temperature program desorption measurements there are also two desorption pathways of sulfur adsorbed from the gas phase[29] (see Introduction). We connect the S adsorbate electrooxidized at 0.70 V with desorption of S_2 molecules from the bridge surface sites since the oxidation and thermal desorption features appear only at high coverage (ca. 1 monolayer). These bridge sites are evidently easy to nucleate by the oxygen-donating water in reaction 1. The broad range sulfur oxidation is therefore concluded to result from the hollow Pt(111) sites.

AES and CEELS Data. Typical Auger wide range electron spectra from the clean and sulfur-covered Pt(111) surfaces are

(53) Ertl, G.; Kuppers, J. *Low Energy Electrons and Surface Chemistry*; Weinheim, VCH: Deerfield Beach, FL, 1985; pp 220−222.

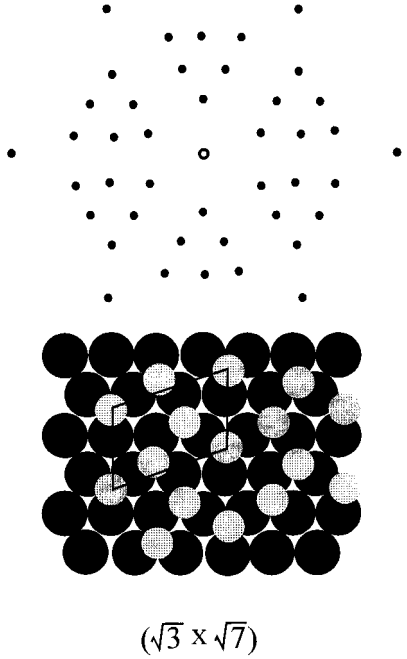

Figure 3. Diagram of the $(\sqrt{3}\times\sqrt{7})$ LEED pattern and corresponding surface structure after sulfur adsorption from 1.0 mM NaHS.

shown in Figure 4A. The high-resolution S(LMM) spectral region at 153.0 eV is shown in Figure 4B. The data demonstrate that sulfur is the only surface species, eliminating the possibility of sulfur coadsorption with bisulfate, or surface oxidation. Since the sodium AES signal was not observed either, the sulfur layer appears to be predominantly neutral. However, as we will demonstrate below, there is a negative charge residing on the adsorbate. AES data are also presented for the Na_2S film (Figure 4, see Experimental Section). The AES line shape and peak position for the Na_2S film agree with the Auger electron spectra previously obtained from several sulfides,[54,55] and closely resemble those from sulfur monolayers observed in this study. The ~5 eV shift toward higher kinetic energy in surface sulfur vs that of the Na_2S film is due to the extramolecular relaxation

(54) (a) Bernett, M. K.; Murday, J. S.; Turner, N. H. *J. Electron Spectrosc. Relat. Phenom.* **1977**, *12*, 375−393. (b) Turner, N. H.; Murday, J. S.; Ramaker, D. E. *Anal. Chem.* **1980**, *52*, 84−92.

(55) Sickafus, E. N.; Steinrisser, F. *J. Vac. Sci. Technol.* **1973**, *10*, 43−46.

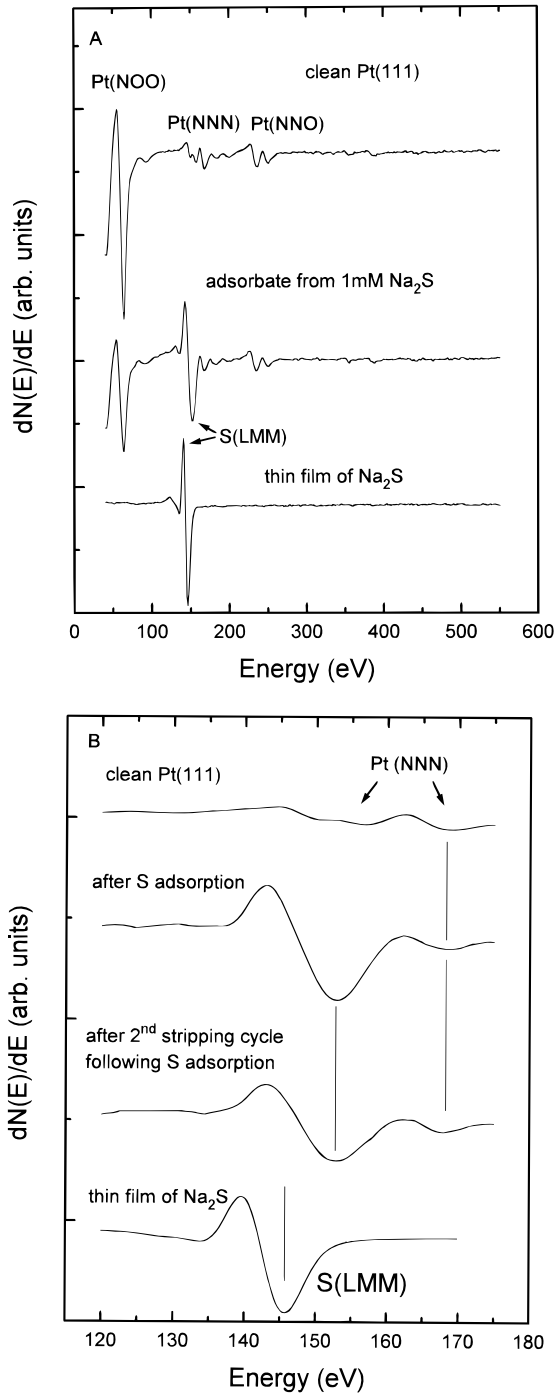

Figure 4. Auger electron spectra (AES) at 3 keV primary beam energy. (A) spectra in the range of 50−550 eV [from top to bottom: data for clean Pt(111), Pt(111) covered by chemisorbed sulfur and by thin film of Na_2S (see Experimental Section)]; (B) spectra from 120 to 175 eV for clean platinum and S-covered platinum before the oxidative voltammetry and after the second voltammetric cycle.

energy effect discussed previously.[40,45,56] As is well-known, the Auger sulfur spectra originate from the $L_{II}M_IM_{II,III}$ and $L_{II}M_{II,III}M_{II,III}$ processes[57] and from cross electron transitions.[58] The maximum coverage obtained from AES (0.95 ± 0.04 monolayer) compares well to that from CV (0.94 ± 0.05 monolayer) (Tables 1 and 2). In agreement with the CV results, the AES coverage obtained using NaHS working solution as the dosing medium is lower than that from Na_2S, 0.70 ± 0.04 monolayer. The data show that even after 20 sweeps a small amount of sulfur still resides on the surface (0.02 monolayer). The cross-referenced data (CV versus AES and LEED, see Tables) are uniquely consistent, reflecting the robustness of the sulfur system upon the electrode emersion and UHV interrogation.

Some more electron spectra[43,59,60] are shown in Figure 5. Figure 5A shows spectra in both AES and CEELS regions. In Figure 5B, CEEL spectra presented both in the differentiated and integrated mode are scrutinized. The main core loss feature at 165.3 eV is attributed to electron transition from S 2p to the empty level above the Fermi level, the S 3d level.[60] The energy gap between S 2p−S 3d energies obtained from theoretical studies[60] is very close to what we observe experimentally. The additional loss feature at 174.0 eV (Figure 5B) may derive either from the core-level energy-attenuated electron additionally scattered on valence electrons or from the energy transition to a higher level than 3d.[45,60] For the S-adsorbate and thin Na_2S film, the energy loss peaks are at 165.3 and 164.0 eV, respectively, showing that the main loss energy of the adsorbate is higher by 1.3 eV than that from Na_2S. This provides evidence that sulfur is, to a large extent, adsorbed in an atomic form.[6] However, the corresponding S 2p binding energy difference between elemental sulfur and Na_2S from XPS is higher, 2.2 eV,[61] indicating that the S adlayer on the Pt(111) electrode also has some anionic character. This is mainly a consequence of the electron transfer from platinum to sulfur, for instance Pt 5d to S sp for the hollow-site bound sulfur.[29] Notably, when sulfur adsorption was carried out from Na_2S solutions containing traces of oxygen (see above), approximately 0.07 monolayer of surface oxygen was found (Figure 6A). CEELS studies show that both the main S 2p loss at 165.3 eV and the additional loss at 174.0 eV are common to both oxygen-free and oxygen-containing adsorbates (Figure 6B). However, the relative intensity of the two energy transitions and the morphology of the loss peak at 174.0 eV are different. Since we eliminated the possibility that the spectrum is due to surface sulfate or to oxygen coadsorbed with sulfur, we may postulate that a SO_x species is present on the surface, together with sulfur adatoms. Whereas the characterization of this species requires more involved spectroscopic study we emphasize that SO_x must be rigorously avoided if high coverage (≈1 monolayer) sulfur structure is to be found upon electrochemical adsorption conditions.

Finally, in clear contrast to our recent data obtained with bisulfate adsorbate,[45] the S 2p loss energy does not depend on the electrode potential. We connect this difference to the fact that the Pt−HSO_4^- bond is mainly ionic and the Pt−S mainly covalent. Details of this correlation need yet to be worked out.

The Effect of Sulfur on Adsorption of Hydrogen. Positive-going CV profiles of the S-covered Pt(111) electrode taken in the hydrogen region at several sulfur coverages,[11] from 0.0 to 0.94 monolayer, are shown in Figure 7A. The hydrogen coverage is plotted as a function of sulfur coverage in Figure 7B. Between 0.1 and 0.3 monolayer, which corresponds to the appearance of p(2×2) and $(\sqrt{3}\times\sqrt{3})R30°$ structures in LEED experiments, and to hollow-site sulfur adsorption from the data obtained by other investigators,[29] the H−S coverage slope is not far from 1 (Figure 7B). This shows that one sulfur blocks

(56) Briggs D.; Riviere, J. C. In *Practical Surface Analysis*, 2nd ed.; Vol. 1: *Auger and X-ray Photoelectron Spectroscopy*; Briggs, D., Seah, M. P., Eds.; John Wiley & Sons: New York, 1990; pp 85, 201−255.
(57) Farell, H. H. *Surf. Sci.* **1973**, *34*, 465−469.
(58) Weissmann R.; Muller, K. *Surf. Sci. Rep.* **1981**, *1*, 251−309.
(59) Bendazzoli, G. C.; Palmieri, P. *Theor. Chim. Acta* **1974**, *36*, 77−86.
(60) Hitchcock, A. P.; Brion, C. E. *Chem. Phys.* **1978**, *33*, 55−64.
(61) Moulder, J. F.; Stickle, W. F.; Sobol, P. E.; Bomben, K. D. In *Handbook of X-ray Photoelectron Spectroscopy*; Chastain, J., Ed.; Physical Electronics Industries, Inc.: Eden Prairie, MN, 1992; pp 235−236.

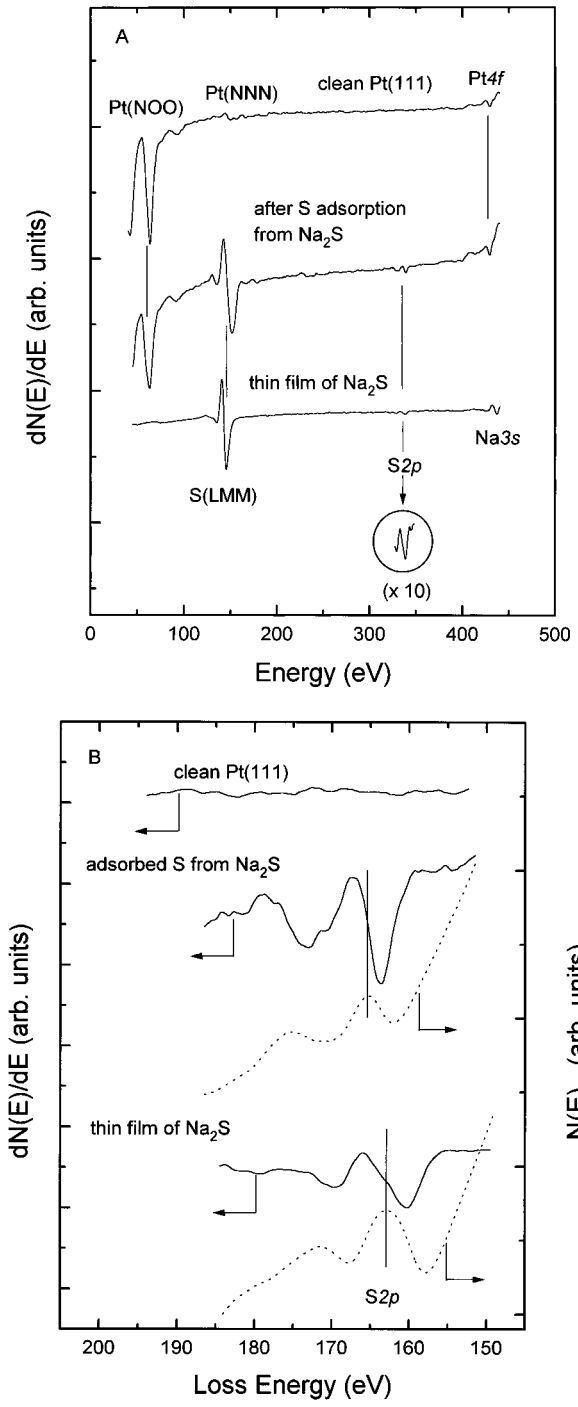

Figure 5. Electron spectra at 500 eV primary beam energy: (A) Pt(NOO), Pt(NNN), and S(LMM) Auger electron transitions and Pt $4f_{7/2}$, S 2p, and Na 3s core level energy loss regions; (B) core level energy loss spectra for S-adsorbate and thin Na_2S film. Shown are spectra as obtained (solid lines) and integrated (dotted lines). Spectra B bottom: AES data for thin Na_2S film.

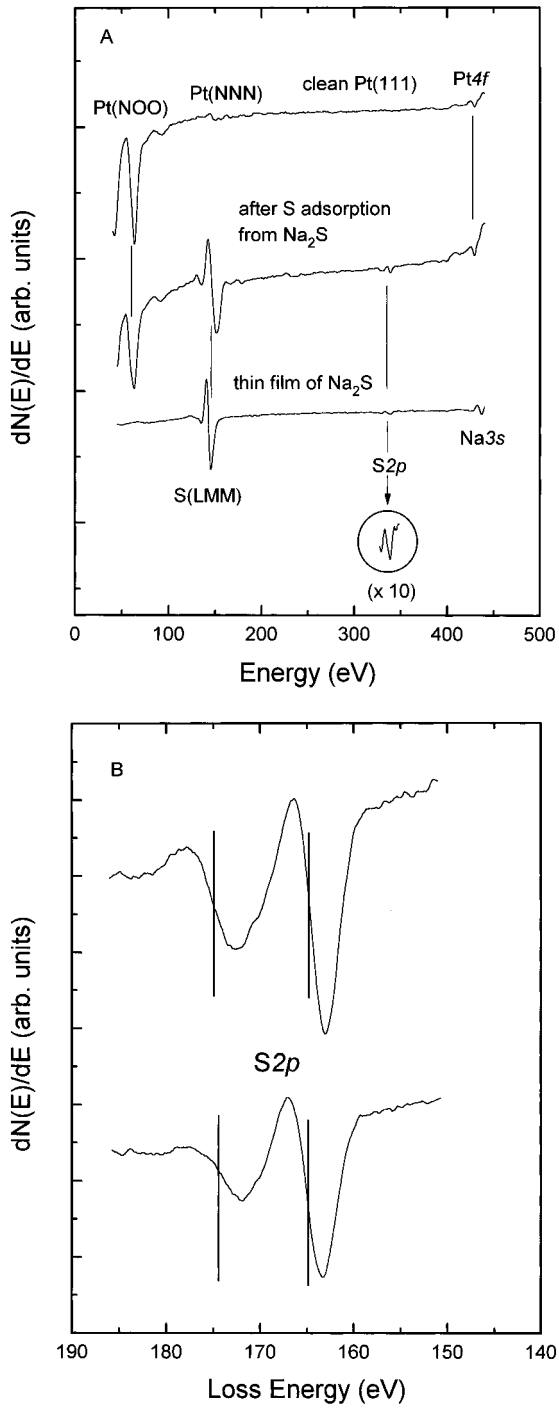

Figure 6. Comparison of electron spectra obtained using deaerated (upper curves) and aerated (lower curves) 1 mM Na_2S solutions for sulfur adsorption at open circuit on Pt(111): (A) Auger electron spectra (at 3 kV); (B) S 2p electron energy loss spectra (at 500 eV).

approximately one surface site as predicted by a simple surface blocking model. Higher coverage than 0.3 monolayer is much more inhibitive, the observation we relate to the bridge-site sulfur adsorption. This is a clearly an electrostatic effect since the charge residing on the bridge-bonded (or atop) sulfur is higher than that on the hollow-site sulfur.[29] Arguably, hydronium cations are electrostatically held at such negatively charged surface sites and the discharge reaction—needed for hydrogen adsorption—is suppressed.

At the lowest sulfur coverage, below 0.1 monolayer, one surface sulfur adatom is capable of blocking as many as 10 ± 1 platinum atoms (Figure 7B). Marcus and Protopopoff have already demonstrated the sulfur-induced, site-blocking effects in hydrogen adsorption on a Pt(111) electrode.[11] While there is a general agreement between their work and ours, there are also some differences. The quoted authors observed that adsorption of hydrogen was totally inhibited at 0.36 monolayer (and at higher S coverage) while our data show that there is still ca. 5% hydrogen accommodated by the surface. At S coverage lower than 0.17 monolayer, our data show somewhat higher hydrogen suppression than in Marcus and Protopopoff's profiles. However, at the lowest hydrogen coverage, Marcus and Protopopoff obtained the number of hydrogen adsorption

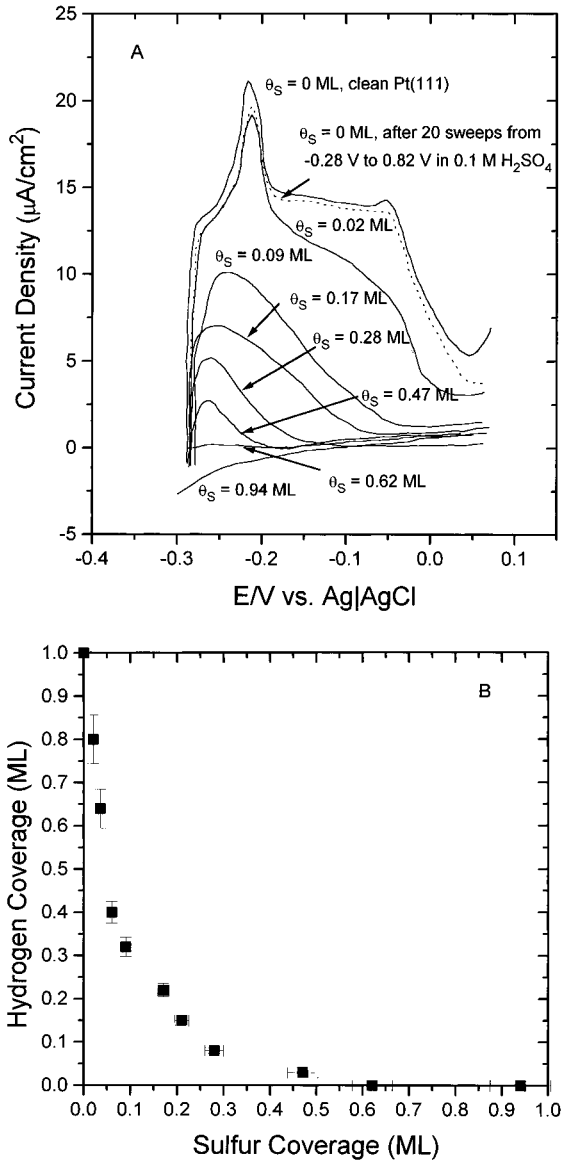

Figure 7. The effect of sulfur on adsorption of hydrogen on Pt(111): (A) voltammetric profiles for hydrogen desorption at the indicated sulfur coverage in 0.1 M H_2SO_4 solution; (B) the plot of hydrogen coverage versus sulfur coverage (in monolayers).

sites blocked by one sulfur atom equal to 8 ± 1, not far off from our data: 10 ± 1.

To explain the excessive blocking effect at low coverage, a coadsorption model was proposed[11] where a single S atom blocks all sites in the nearest-neighbor position to the sulfur atom. This would lead to deactivation of 7 rather than 10 platinum atoms. Without rejecting the previous model, an alternative explanation could again highlight the significance of the dipole moment formed due to the Pt → S electron transfer. On a scarcely populated surface free of depolarization effects, the electrostatic interactions are likely to extend well beyond the nearest-neighbor platinum atoms, thus stabilizing large water−proton clusters and suppressing the electrochemical discharge. Another possibility is, however, that surface sulfur at low coverage has a high degree of 2D mobility to create a dynamic surface state with participation of metal electrons and coadsorbed hydrogen atoms. An access into such a tentatively proposed dynamic configuration requires dedicated *in situ* surface analyses that have been initiated in this laboratory.

4. Conclusions

Our observations are important for several reasons. First, we found that electrooxidation of surface sulfur may occur in the form of a narrow voltammetric spike in the potential range preceding surface oxidation. Second, we found a series of surface structures depending on sulfur coverage, (1×1), (2×2) at $^1/_2$ monolayer, ($\sqrt{3}\times\sqrt{7}$), ($\sqrt{3}\times\sqrt{3}$)*R*30° to p(2×2) at $^1/_4$ monolayer, and a low coverage (2×2). Such a rich structural chemistry has not yet been reported before in electrochemical research. Third, we provided evidence that a negative charge resides on the Pt(111)-bound S adsorbate. Fourth, we connected sulfur chemical state observations to a nonlinear suppression effect that S adsorbate exerts on hydrogen adsorption. Fifth, we showed evidence that oxygen is permanently incorporated in the S adsorbate if sulfur adsorption takes place in solutions containing traces of atmospheric oxygen. In summary, we believe our studies provide a detailed picture of sulfur adsorption on Pt(111), connect the structure with typical forms of electrochemical reactivity, and highlight the need for an oxygen-free environment for studies with S adsorbates in electrochemistry. We also believe that due to high room temperature stability in both aqueous solutions and vacuum, the structure of chemisorbed sulfur can successfully be investigated by electron spectroscopies and electron diffraction in UHV. The advantage of these techniques is that they reveal surface structure, coverage, and chemical state in a single solution−vacuum emersion experiment. Insights in electron charge transfer and surface motion events need then be added through *in situ* research.

Acknowledgment. This work is supported by the National Science Foundation, under Grant CHE 94-11184, and by the Department of Energy, under Grant DE-AC02-76ER01198, administrated by the Frederick Seitz Research Laboratory at the University of Illinois at Urbana−Champaign. G. Jerkiewicz acknowledges Research Grants from the NSERC of Canada and the FCAR du Québec.

Supporting Information Available: LEED patterns from Pt(111) surfaces: (1×1) from clean Pt, (1×1) at ~1 monolayer of sulfur after adsorption from 1 mM Na_2S, (2×2) at $^1/_2$ monolayer of S after the first voltammetric cycle, ($\sqrt{3}\times\sqrt{3}$)*R*30° at $^1/_3$ monolayer of S after the seconds cycle, and p(2×2) at $^1/_4$ monolayer of S after the third cycle (3 pages). See any current masthead page for ordering and Internet access instructions.

JA962637H